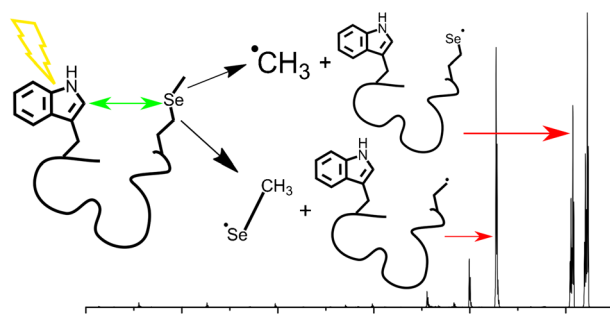


Methionine and Selenomethionine as Energy Transfer Acceptors for Biomolecular Structure Elucidation in the Gas Phase

Lance E. Talbert, Ryan R. Julian 

Department of Chemistry, University of California, Riverside, 501 Big Springs Road, Riverside, CA 92521, USA



Abstract. Mass spectrometry affords rapid and sensitive analysis of peptides and proteins. Coupling spectroscopy with mass spectrometry allows for the development of new methods to enhance biomolecular structure determination. Herein, we demonstrate two new energy acceptors that can be utilized for action-excitation energy transfer experiments. In the first system, C–S bonds in methionine act as energy acceptors from native chromophores, including tyrosine,

tryptophan, and phenylalanine. Comparison among chromophores reveals that tyrosine transfers energy most efficiently at 266 nm, but phenylalanine and tryptophan also transfer energy with comparable efficiencies. Overall, the C–S bond dissociation yields following energy transfer are low for methionine, which led to an investigation of selenomethionine, a common analog that is found in many naturally occurring proteins. Sulfur and selenium are chemically similar, but C–Se bonds are weaker than C–S bonds and have lower lying σ^* anti-bonding orbitals. Excitation of peptides containing tyrosine and tryptophan results in efficient energy transfer to selenomethionine and abundant C–Se bond dissociation. A series of helical peptides were examined where the positions of the donor or acceptor were systematically scanned to explore the influence of distance and helix orientation on energy transfer. The distance was found to be the primary factor affecting energy transfer efficiency, suggesting that selenomethionine may be a useful acceptor for probing protein structure in the gas phase.

Keywords: FRET, Action spectroscopy, Distance constraint, EET, Photodissociation, Ion mobility

Received: 1 May 2019/Revised: 31 May 2019/Accepted: 1 June 2019/Published Online: 20 June 2019

Introduction

There is significant interest in the development of new methodology for the characterization of biological molecules in both a rapid and sensitive fashion. Mass spectrometry (MS) offers an avenue to accomplish these goals and, as such, has been used extensively for protein identification, sequencing, and quantitation.^{1–5} MS technology is now widely available due to the popularity of proteomics, which has spurred efforts to develop methods capable of higher-order structure determination. Ion mobility-MS is the most commonly used gas phase method capable of providing information about three-dimensional structure.^{6–12} Ion mobility yields structural

data in the form of averaged collision cross section for each ion. Ion mobility is fairly easy to implement and can examine a wide range of molecular targets, but it is not always possible to completely constrain molecular structure with a single parameter. Recent developments have expanded the parameter space of ion mobility by examining cross sections as a function of activation, which can provide clues about substructural elements and organization.¹³

Spectroscopy can also be coupled with MS for structural characterization, including both ultraviolet (UV)- and infrared (IR)-based approaches.^{14, 15} Common condensed-phase techniques like Förster Resonance Energy Transfer (FRET) can be employed to obtain structural information about the peptide or protein of interest. Traditional FRET reveals the distance between a donor and acceptor, typically between 10 and 100 Å, by exciting the donor and monitoring emission of the

Correspondence to: Ryan Julian; e-mail: ryan.julian@ucr.edu

acceptor.¹⁶ Work by the Jockusch and Zenobi groups has demonstrated that the FRET-based approach with fluorescence detection can be successfully implemented in the gas phase within the confines of a mass spectrometer.^{17–19} It is also possible to utilize action spectroscopy-based experiments in a mass spectrometer where absorption of photons is assumed to correlate with ion dissociation. Action spectra are generated by scanning the excitation wavelength while monitoring fragment intensity. By coupling energy transfer with action spectroscopy, donor/acceptor distance constraints can be determined without detecting photons directly.²⁰ Dugourd and coworkers have used this approach to examine small peptides and ubiquitin, modified with FRET chromophores.^{21, 22}

Our lab has developed an action spectroscopy system that relies on native chromophoric amino acids as donors and propyl mercaptan (PM)-modified cysteine as the acceptor. Energy transfer in this system occurs over short distances, smaller than the typical range for FRET, so the more general term excitation energy transfer (EET) has been used to describe the experiment. Excitation of peptides containing either tyrosine or tryptophan yields minimal nonspecific fragmentation at 266 nm. However, if either residue is spatially located near a PM-modified cysteine, energy transfer to the disulfide results in homolytic cleavage in a distance-dependent fashion.^{23, 24} Experiments with molecules of a known structure revealed that energy transfer can occur at < 15 Å for tryptophan and < 6 Å for tyrosine. Phenylalanine, while aromatic, does not directly transfer energy to disulfide bonds efficiently. However, phenylalanine can participate in a two-step process where energy transfer passes through an intermediary tyrosine residue.²⁵ Recently, Rizzo and coworkers also examined energy transfer from electronically excited phenylalanine to tyrosine in a cryogenic trap.²⁶ This system represents a close analog of the action-EET experiments we have conducted, and it was determined that energy transfer is best represented by the full Coulomb interaction between the donor and acceptor. The dipole-based FRET approximation was insufficient to describe the results, and Dexter exchange pathways were found to be negligible.

The addition of propyl mercaptan to a free thiol on cysteine is a mild and relatively easy-to-carry-out modification, but one that becomes more challenging with increasing protein size and complexity. The presence of native disulfides can introduce the potential for disulfide scrambling, particularly if the protein does not have cysteine in the free-thiol state natively, which is not particularly common. This prompted an investigation into other native amino acids that could act as acceptors in an entirely native action-EET system. Recently, we reported that 213 nm photons homolytically cleave C–S bonds in both cysteine and methionine.²⁷ Although S–S bonds are inherently cleavable, photolysis of C–S bonds is not typically observed at 266 nm unless the C–S bond comprises part of a more suitable chromophore.^{28, 29} However, the 213 nm experiments revealed that C–S bonds harbor dissociative electronic excited states that might be accessible via energy transfer under appropriate conditions.

Methionine therefore warrants additional attention because it contains C–S bonds but not disulfide bonds and is not subject

to disulfide scrambling. It is an essential amino acid in humans and the most common start codon for protein synthesis. Methionine can also behave as an antioxidant.^{30, 31} A common amino acid analog of methionine, selenomethionine (SeMet), also exists in nature and only differs by a single atom, selenium in place of sulfur. SeMet is also biologically relevant and is the major dietary source of selenium for many living organisms, where selenium is both essential and toxic. Uptake of SeMet is typically followed by conversion to selenocysteine, the 21st amino acid, and incorporation into proteins.³² SeMet is also routinely incorporated abiologically into proteins for phasing in X-ray crystallography.^{33, 34} Sulfur and selenium share many physical and chemical properties including similar electronegativity, ionic radii, and bond length.³⁵ Important chemical differences include the following: carbon–selenium bonds are weaker than carbon–sulfur bonds, and they have lower-lying σ^* anti-bonding orbitals.³⁶ These differences in bonding could lead to significantly altered energy transfer efficiency.

Herein we examine the potential for Met and SeMet to act as native amino acid energy transfer acceptors. Data on model peptides shows that both C–S bonds in Met dissociate following energy transfer from all three aromatic amino acid donors: phenylalanine, tyrosine, and tryptophan. Energy transfer is most efficient for tyrosine, followed by phenylalanine and then tryptophan. While energy transfer is observed, C–S bonds are generally poor energy acceptors and can only accommodate low PD yields. In contrast, C–Se bond dissociation following energy transfer to SeMet is significantly more abundant. Donor efficiency for SeMet follows the order Trp>Tyr>>Phe. To further explore the structure probing capabilities of SeMet, a series of helical peptides were synthesized where the relative donor/acceptor positions were systematically varied. The trends in bond dissociation followed the characteristic pattern expected for a helical peptide, confirming that SeMet is a viable acceptor for probing peptide structure in the gas phase.

Experimental Methods

Materials and Peptide Synthesis

Methanol was purchased from Fisher Scientific (Waltham, MA). Water was purified by Millipore Direct-Q (Millipore, Billerica, MA). Fmoc-SeMet was purchased from Matrix Scientific (Columbia, Sc). Polyalanine peptides were synthesized with the following sequences: Ac-A₅XA₃MK and Ac-A₅XA₃M^{Se}K (where X = Y, F, or W), A₃MK, and A₃M^{Se}K. Additionally, a series of SeMet helical peptides were synthesized containing either tyrosine or tryptophan with the following sequences: Ac-XA₈M^{Se}K, Ac-AXA₇M^{Se}K, Ac-A₂XA₆M^{Se}K, Ac-A₃XA₅M^{Se}K, Ac-A₄XA₄M^{Se}K, Ac-A₅XA₃M^{Se}K, (X = Y or W). A series of peptides with tryptophan near the C-terminus were also made with the following sequences: Ac-M^{Se}A₈WK, Ac-AM^{Se}A₇WK, Ac-A₂M^{Se}A₆WK, Ac-A₃M^{Se}A₅WK, Ac-A₄M^{Se}A₄WK, and Ac-A₅M^{Se}A₃WK. Peptides were synthesized following the standard solid phase peptide synthesis procedures for most amino

acid additions.³⁷ The coupling and deprotection steps were completed in 6 min for all amino acids except SeMet, for which coupling was extended to 1.5 h.

Photodissociation of Peptides

A linear ion trap (LTQ) mass spectrometer (Fisher Scientific, Waltham, MA) with a standard ESI source was utilized for photodissociation experiments. A quartz window was installed on the back plate of the LTQ for transmission of laser pulses from a flash-lamp pumped Nd:YAG Minilite laser (Continuum, Santa Clara, CA). A single 266-nm pulse from the 4-mJ laser was synchronized to occur at the activation step of the MS² experiment, triggered by the instrument. Peptides were dissolved in 50:50 water:MeOH in 0.1% TFA at 10 μ M concentrations and electrosprayed at 3 μ L/min with a voltage of 3.25 kV and a capillary inlet temperature set to 215 $^{\circ}$ C.

For action-EET experiments, an optical parametric oscillator (OPO) laser (Opotek Inc., Carlsbad, CA) was utilized. Ions were isolated and subjected to a single laser pulse at wavelengths varying from 250 to 300 nm. Laser power levels for each wavelength were recorded and normalized. The OPO laser power is typically one-fourth of the Nd:YAG at 266 nm, which is reflected when comparing the PD yields between the two setups. Action spectra were compiled using the PD yield at each wavelength. Instrument and peptide conditions were the same as the 266 nm photodissociation experiments described above.

Simulated Annealing and Molecular Dynamics Simulations

Simulated annealing and molecular dynamics (MD) simulations were performed with MacroModel (Schrödinger Inc., Portland, Oregon) using the OPLS2005 atomic force fields. Simulated annealing was first performed by heating the starting structure up to 1000 K and then slowly cooled to 200 K. This process was repeated until 1000 structures were obtained yielding a population of potential structures. The lowest energy structure was selected, and a subsequent MD simulation was performed. For the simulation, 1000 structures were obtained under the following conditions: 300 K with a 1.0 ps equilibration time, 1.5 fs step time, and a 5 ns simulation time. To estimate the distance between the donor and acceptor, distances were measured from all atoms located on the aromatic rings, of either tyrosine or tryptophan, to one of the two carbon atoms adjacent to selenium in the SeMet side chain (CH₃-Se/Se-CH₂) as well as to the selenium atom. The distances were sorted and the shortest distances were averaged to represent the closest point of contact for each 1000 structure MD simulation.

Results and Discussion

To test the feasibility of energy transfer to the C–S bonds of methionine, helical peptides with the sequence Ac-A₅XA₃MK were synthesized where X was tyrosine, tryptophan, or

phenylalanine. These peptides have been well characterized in previous studies to maintain their alpha-helical structure during the transition from liquid to the gas phase and place the chromophore in close proximity to the position occupied by methionine.^{23, 38} Figure 1a and b show excitation at 266 nm of the tyrosine and tryptophan containing helical peptides, respectively. Ac-A₅YA₃MK primarily dissociates at the methionine

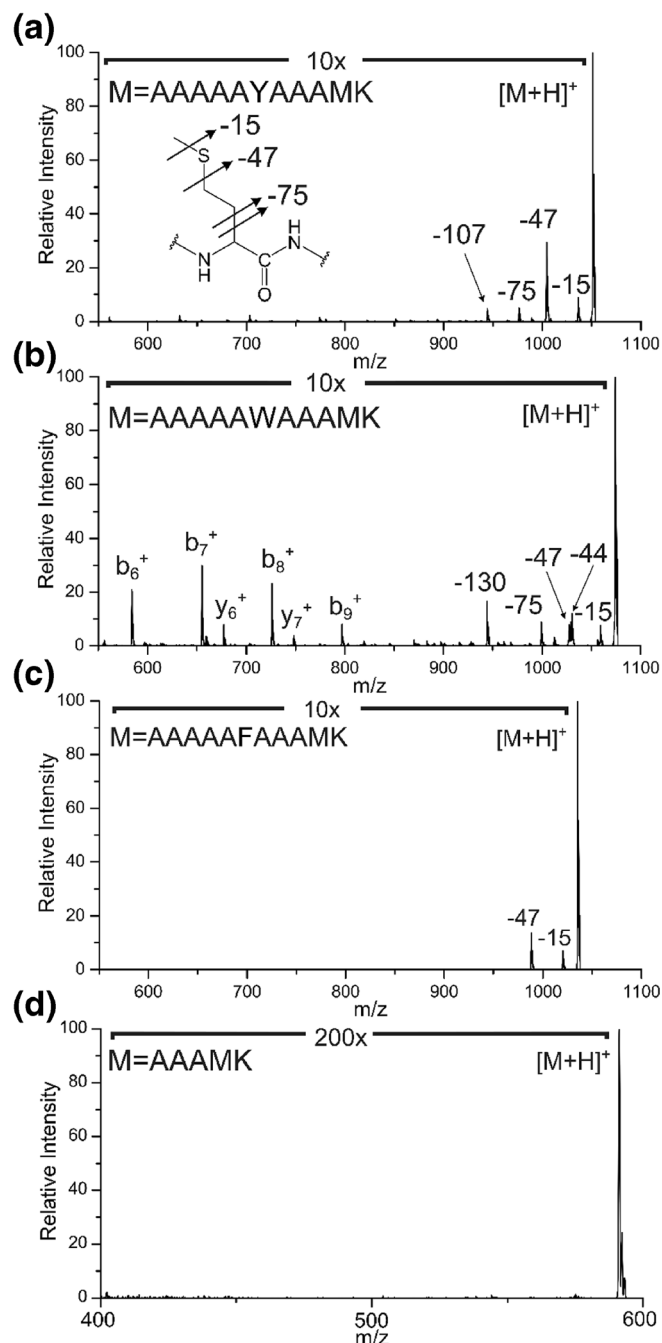


Figure 1. Photoactivation of A₅XA₃MK peptides at 266 nm, where X is (a) tyrosine, (b) tryptophan, or (c) phenylalanine. The fragmentation pathways for the methionine side chain are shown in the inset graphic, where a double arrow indicates a sequential double loss. (d) PD of A₃MK with no observable methionine side chain dissociation

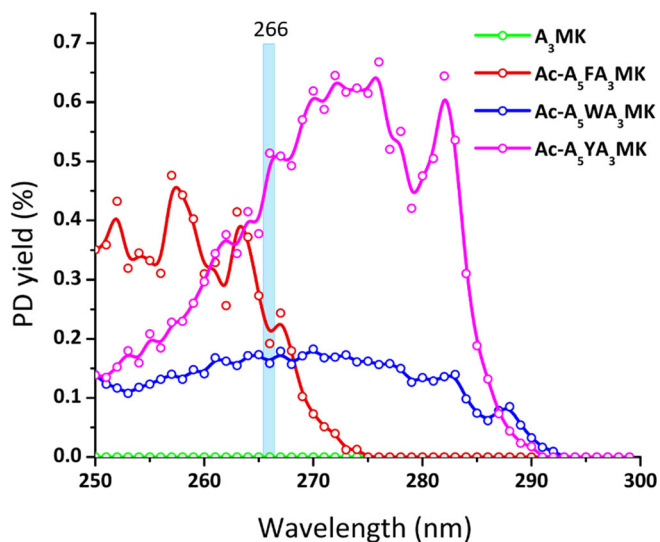


Figure 2. Action spectra representing the sum of -15 Da and -47 Da losses for each respective peptide

side chain C–S bonds, yielding mass losses of -15 and -47 Da. The loss of -75 Da represents a secondary product ion formed following the loss of ethylene from the original -47 Da product ion. The loss of -107 Da is not related to energy transfer and results from direct dissociation of the bond connecting the tyrosine side chain. Analogous results (where -130 Da corresponds to the tryptophan side chain loss) are obtained for Ac-A₅W_A₃MK with additional fragments including loss of CO₂ and a series of b- and y-ions. The sequence ions result from the internal conversion of the photon energy into heat. The CO₂ loss (-44 Da) likely results from hydrogen atom abstraction from the C-terminal $-\text{COOH}$.³⁹ Figure 1c shows the results for 266 nm excitation of Ac-A₅F_A₃MK. Interestingly, the dissociation of the methionine side chain is observed. While phenylalanine is a weak chromophore at 266 nm, there is sufficient absorption and energy transfer to the C–S bonds in methionine to clearly generate the -15 and -47 Da losses.²⁵ The secondary loss of -75 Da is not observed, which may suggest that no additional photons are absorbed by phenylalanine. Photoactivation of a peptide containing no aromatic residues, A₃MK, is shown in Figure 1d. No dissociation of the methionine side chain is observed, indicating that the C–S bonds do not absorb 266 nm photons on their own.

To explore whether the dissociation observed in Figure 1 was due to energy transfer, action spectra were collected and are shown in Figure 2. The PD yields are a summation of the two primary losses (-15 and -47 Da) that result from excited-state C–S bond cleavage. The spectra clearly reflect the characteristic features for the absorption of phenylalanine, tyrosine, and tryptophan in the range of 250–300 nm.⁴⁰ The pink trace exhibits the two characteristic peaks for tyrosine between 275 and 285 nm, while the blue trace for tryptophan is broader with two distinctive features at 283 and 287 nm. The red trace shows a triplet of peaks between 250 and 265 nm that correspond well with the known absorption profile for phenylalanine. In contrast, the methionine-only peptide (green trace) does not yield

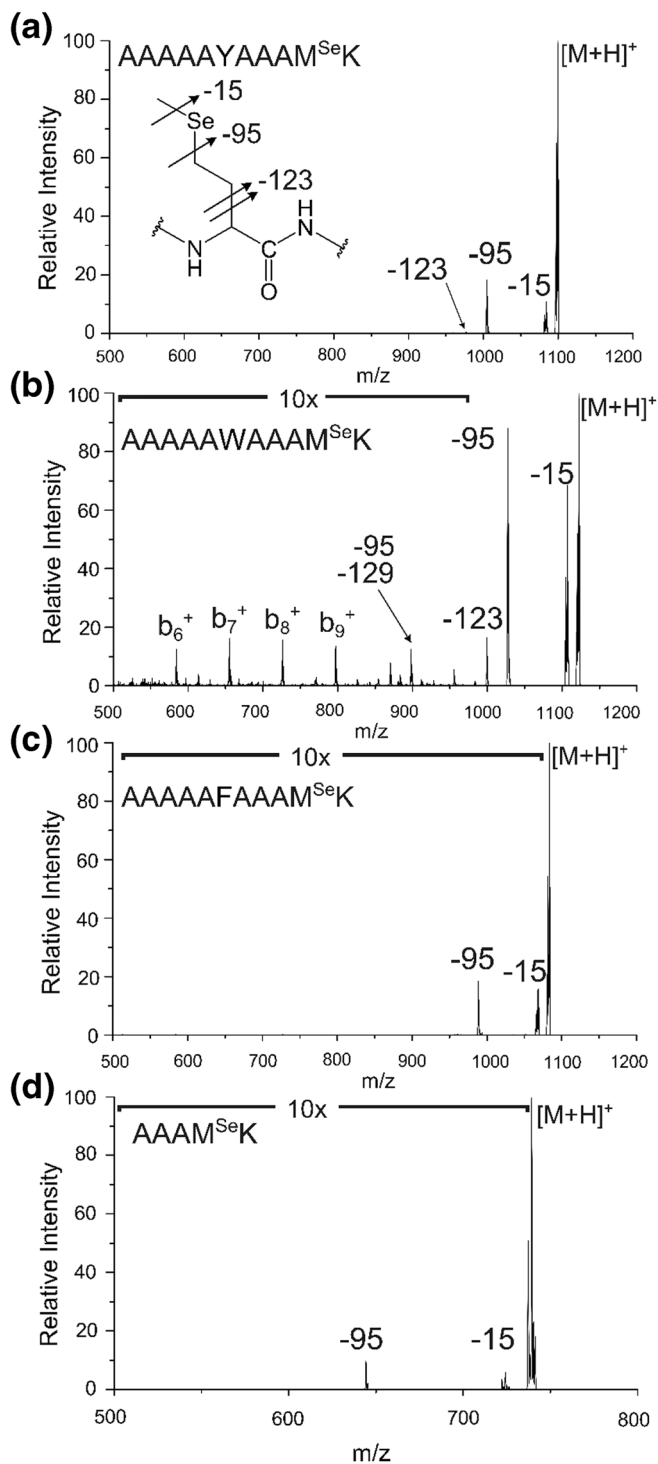


Figure 3. Photoactivation of Ac-A₅X_A₃M^{Se}K peptides at 266 nm, where X is (a) tyrosine, (b) tryptophan, or (c) phenylalanine. (d) Same experiment with A₃M^{Se}K

any appreciable amount of C–S bond cleavage. The action spectra in Figure 2 provide strong evidence that dissociation of C–S bonds in these peptides is due to energy transfer. From the perspective of PD yield, tyrosine is the most efficient energy donor at 266 nm, while Trp and Phe only net approximately half the energy transfer of Tyr. Overall, energy transfer

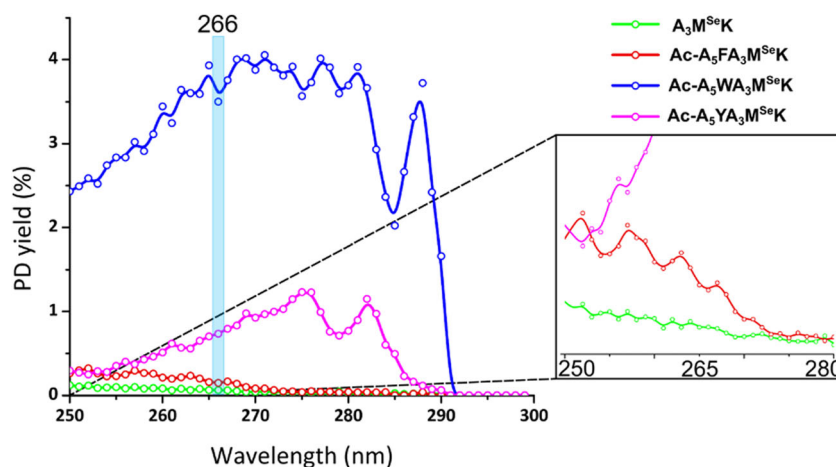


Figure 4. Action spectra showing the sum of -15 Da and -95 Da losses for each respective peptide

to methionine is not particularly efficient and the PD yields for all chromophores are small. Although this does not present a problem for the examination of small peptide systems, it is not optimal as molecular scale increases to larger proteins where many other competing fragmentation pathways, though they may also be minor, are likely to compete.

Given the limited success of C–S bonds as energy acceptors for action-EET, we explored alternative forms of methionine to see if more abundant energy transfer and PD yield could be achieved. Figure 3 shows the results for photoexcitation of a series of synthetic helical peptides incorporating SeMet into the generic sequence $\text{Ac-A}_5\text{XA}_3\text{M}^{\text{SeK}}$, where X = tyrosine, tryptophan, or phenylalanine. Fragments analogous to those observed for methionine are also detected for SeMet, but the PD yields are much higher for Tyr and Trp ($\sim 10\times$ for Tyr, $\sim 80\times$ for Trp). However, energy transfer from Phe to SeMet does not appear to be a favorable process and yields minimal C–Se bond dissociation. The relative amount of backbone fragmentation to side chain fracture is significantly less for $\text{Ac-A}_5\text{WA}_3\text{M}^{\text{SeK}}$ compared with its methionine counterpart in Figure 1b. This also suggests more efficient energy transfer to C–Se bonds, resulting in less vibrational excitation following internal conversion. Examination of the $\text{A}_3\text{M}^{\text{SeK}}$ peptide reveals that, in the absence of aromatic residues, only slight dissociation of C–Se bonds is observed. Overall, energy transfer to C–Se bonds appears to be much more favorable than what is observed in methionine C–S bonds.

Figure 4 shows the action spectra collected between 250 and 300 nm for the peptides examined in Figure 3. Again, the action spectrum for each chromophore correlates strongly with the known absorption profile. Even the phenylalanine-containing peptide, despite exhibiting very weak energy transfer, yields a spectrum with the characteristic triplet of peaks (see inset). In contrast, the action spectrum for SeMet itself, as observed in the peptide $\text{A}_3\text{M}^{\text{SeK}}$, reveals no characteristic features and simply decays with increasing wavelength. This is similar to what is observed for the action spectrum of disulfide bonds in the absence of other chromophores. It is likely that the lower-lying C–Se σ^* anti-bonding orbital

facilitates energy transfer from the excited states accessible in this wavelength region, particularly in the case of tryptophan. The greatly increased PD yields for SeMet suggest that it could serve as a viable energy acceptor for structure exploration in proteins if the energy transfer correlates with distance.

To investigate the relationship between C–Se bond energy transfer efficiency and distance, a series of helical peptides containing SeMet and tyrosine were synthesized. The generic sequence corresponds to $\text{Ac-A}_x\text{YA}_y\text{M}^{\text{SeK}}$, where x and y vary from 0–5 to 3–8 in concert, respectively. Individual PD yields for the -15 , -95 , and -123 Da losses are shown in Figure 5a for the entire peptide series. The abundance of the two-step -123 Da loss is low for all peptides. The two losses corresponding to C–Se bond cleavage (-15 and -95 Da) are more abundant and generally comparable in intensity, although some variation is noted. However, the overall intensity of these losses changes significantly as the position of the tyrosine chromophore is scanned through the sequence. Importantly, the intensity drops initially, but then increases again for $\text{Ac-A}_2\text{YA}_6\text{M}^{\text{SeK}}$, which is consistent with the expected distances between Tyr and SeMet for a helical structure. This is illustrated visually for an idealized alpha-helix in Figure 5b from the end-on perspective. To provide quantitative values, distances were measured during molecular dynamics (MD) simulations. Simulated annealing was first used to examine a broad population of potential structures and identify low-energy candidates. The lowest energy structures exhibited alpha-helical motifs in agreement with the data in Figure 5 and previous studies.^{23, 41} Average distances extracted from subsequent MD simulations at 300 K are shown in the inverse form in Figure 5a. Although the relative differences for each peptide do not match exactly, similar trends are observed for the experimentally derived PD yields and the computationally derived inverse distances between residues. These results confirm that the peptide adopts a helical form in the gas phase and that probability for energy transfer to C–Se bonds scales with distance.

The results in Figures 3 and 4 reveal that Trp donates energy more efficiently to C–Se bonds than Tyr. The distance dependence for energy transfer from Trp was examined with an

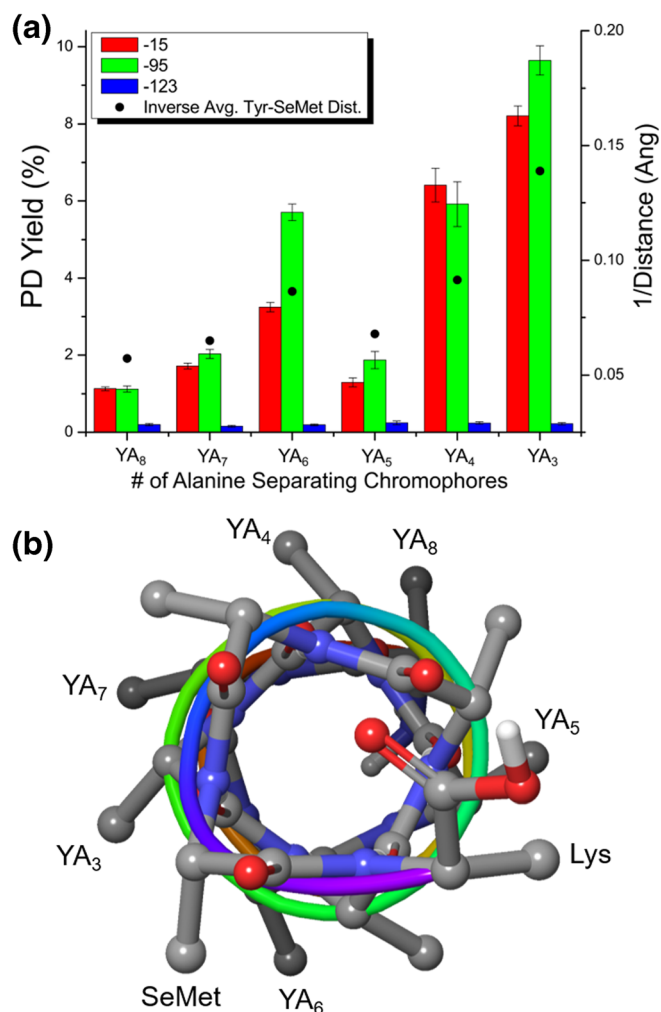


Figure 5. (a) PD yields for $Ac-A_xYA_yM^{Se}K$ peptides, where x and y range from 0–5 to 3–8, respectively. The black dots refer to the inverse of the average distance measured between SeMet and tyrosine obtained from MD simulations. (b) Structure of an alpha-helix, with C-terminus projecting toward the viewer. The positions of Lys and SeMet are labeled and remain fixed for all peptides. The relative position of the tyrosine residue changes for each peptide and is shown with the corresponding YA_y label. It is clear that YA_3 and YA_6 locate SeMet and Tyr in the closest proximity. Error bars represent the standard deviation of the mean

analogous series of peptides, $Ac-A_xWA_yM^{Sc}K$, and the results are shown in Figure 6a. The overall trends in Figure 6a are similar to those obtained previously with Tyr as the donor, but there are several differences as well. Most notably, the overall PD yield is higher for all peptides, suggesting again that energy transfer is more efficient with Trp. In addition, the abundance of the –123 Da sequential loss peak is higher, suggesting that some additional photons are converted into heat. Although the ratio of the –95 to –15 Da peaks occasionally inverts for Tyr, the –95 Da loss is always more abundant for Trp. The factors that account for this difference are not immediately clear. Previous work examining energy transfer between phenylalanine and tyrosine revealed that the relative chromophore

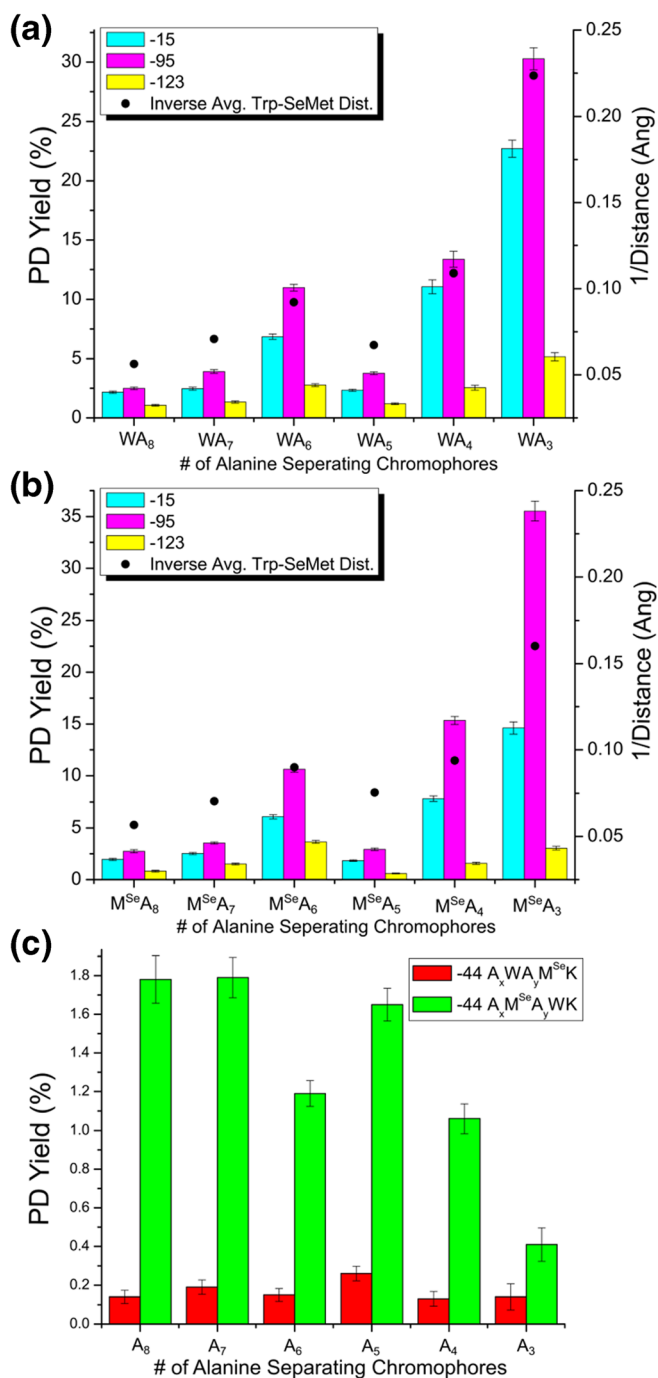


Figure 6. (a) PD yields for tryptophan containing peptides with the sequence of $Ac-A_xWA_yM^{Se}K$, where x and y refer to the number of alanines ranging from 0–5 to 3–8, respectively. (b) PD yields for the reversed $Ac-A_xM^{Se}A_yWK$ peptide series. MD and molecular dynamics simulations were used to obtain the average distance between the tryptophan and SeMet side chains. The inverse of the average distances is plotted as black dots in both (a) and (b). (c) PD yields for the loss of CO_2 observed for the two tryptophan containing peptide series $Ac-A_xWA_yM^{Se}K$ (red) and $Ac-A_xM^{Se}A_yWK$ (green). The x -axis refers to the number of alanines, separating SeMet and tryptophan. Error bars represent the standard deviation of the mean

orientation could influence energy transfer efficiency by roughly a factor of ~ 2 .²⁶ To explore potential orientation effects, we examined the inverted peptide series, Ac-A_xM^{Se}A_yWK, where the position of SeMet was scanned through the helix. The results are shown in Figure 6b. The data in Figures 6a and b are similar, particularly beyond the M^{Se}A₅ position. The orientation of the donor and acceptor to the peptide is reversed between these series, making it likely that the relative orientation or orientations of the donor and acceptor are different as well. If present, these differences do not significantly change the degree of energy transfer as measured in the PD yield. It is possible that this lack of sensitivity to orientation occurs because these ions are at or near room temperature where local dynamic motion may average out such effects. In any case, the data suggest that both Tyr and Trp can be used with SeMet for probing structure by distance-dependent energy transfer.

Placement of Trp next to the C-terminus also increases the loss of -44 Da, corresponding to loss of CO₂. Furthermore, the abundance of the CO₂ loss correlates with donor/acceptor distance in a reciprocal fashion (see Fig. 6c). Essentially, this suggests that excitation of the Trp is quenched by competing pathways, either energy transfer to the SeMet side chain or by reaction with the C-terminus. As the SeMet side chain is moved further away, the probability for reaction with the C-terminus increases. Given that the peptides are all singly charged at the lysine residue with the N-terminus acetylated, the C-terminus is most likely in the $-COOH$ state, necessitating the loss of hydrogen prior to the loss of CO₂. The excited state Trp may abstract a hydrogen atom, similar to previous observations with electronically excited benzophenone.³⁹ Since this is a chemical reaction that may require proper orientation of the Trp sidechain and C-terminus, it is less likely to compete with fast energy transfer when the SeMet sidechain is also in close proximity. However, if Trp is not adjacent to the C-terminus, the probability for CO₂ loss is low and fairly uniform, indicating a pathway independent of direct interaction with the chromophore. Although the data in Figure 6c make it tempting to consider CO₂ loss as an additional potential reporter for structural information, the competing background channel would make it difficult to implement in more complicated systems.

Conclusion

We have examined methionine and SeMet as potential energy acceptors in action-EET experiments. When studying simple helical peptide models, the C–S bonds of methionine can be coupled with tryptophan, tyrosine, and phenylalanine as energy donors. As the complexity and size of the target molecule increases, the low observed yields of C–S bond dissociation may become difficult to observe against the background of more common losses like NH₃ (-17 Da), H₂O (-18 Da), CO₂ (-44 Da), and CO₂H (-45 Da). In contrast, the C–Se bonds from SeMet dissociate with significantly higher yields when adjacent to either tyrosine or tryptophan. A series of helical peptides containing either tyrosine or tryptophan

revealed that energy transfer to SeMet is efficient within ~ 15 Å from the acceptor. Swapping the positions of the donor and acceptor resulted in small changes to dissociation yields, suggesting that orientational effects may not be significant in these room-temperature experiments. Incorporation of SeMet into proteins is not difficult because it is essentially recognized as methionine during protein synthesis in cells.⁴² These experiments pave a path forward for future examination of protein structure in the gas phase by action-EET relying on essentially native amino acid donor/acceptor pairs.

Acknowledgements

The authors gratefully acknowledge funding from the NSF (CHE-1401737) and NIH (R01GM107099).

References

1. Han, X., Aslanian, A., Yates, J.R.: Mass spectrometry for proteomics. *Curr. Opin. Chem. Biol.* **12**, 483–490 (2008)
2. Picotti, P., Clément-Ziza, M., Lam, H., Campbell, D.S., Schmidt, A., Deutsch, E.W., Röst, H., Sun, Z., Rinner, O., Reiter, L., Shen, Q., Michaelson, J.J., Frei, A., Alberti, S., Kusebauch, U., Wollscheid, B., Moritz, R.L., Beyer, A., Aebersold, R.: A complete mass-spectrometric map of the yeast proteome applied to quantitative trait analysis. *Nature*. **494**, 266 (2013)
3. Boersema, P.J., Raijmakers, R., Lemeer, S., Mohammed, S., Heck, A.J.R.: Multiplex peptide stable isotope dimethyl labeling for quantitative proteomics. *Nat. Protoc.* **4**, 484 (2009)
4. Shi, S.D.H., Hemling, M.E., Carr, S.A., Horn, D.M., Lindh, I., McLafferty, F.W.: Phosphopeptide/phosphoprotein mapping by Electron capture dissociation mass spectrometry. *Anal. Chem.* **73**, 19–22 (2001)
5. Cleland, T.P., DeHart, C.J., Fellers, R.T., VanNispen, A.J., Greer, J.B., LeDuc, R.D., Parker, W.R., Thomas, P.M., Kelleher, N.L., Brodbelt, J.S.: High-throughput analysis of intact human proteins using UVPD and HCD on an orbitrap mass spectrometer. *J. Proteome Res.* **16**, 2072–2079 (2017)
6. Bohrer, B.C., Merenbloom, S.I., Koeniger, S.L., Hilderbrand, A.E., Clemmer, D.E.: Biomolecule analysis by ion mobility spectrometry. *Annu Rev Anal Chem (Palo Alto, Calif.)* **1**, 293–327 (2008)
7. Harvey, S.R., MacPhee, C.E., Barran, P.E.: Ion mobility mass spectrometry for peptide analysis. *Methods*. **54**, 454–461 (2011)
8. Bush, M.F., Hall, Z., Giles, K., Hoyes, J., Robinson, C.V., Ruotolo, B.T.: Collision cross sections of proteins and their complexes: a calibration framework and database for gas-phase structural biology. *Anal. Chem.* **82**, 9557–9565 (2010)
9. McLean, J.A., Ruotolo, B.T., Gillig, K.J., Russell, D.H.: Ion mobility–mass spectrometry: a new paradigm for proteomics. *Int. J. Mass Spectrom.* **240**, 301–315 (2005)
10. Pierson, N.A., Chen, L., Valentine, S.J., Russell, D.H., Clemmer, D.E.: Number of solution states of bradykinin from ion mobility and mass spectrometry measurements. *J. Am. Chem. Soc.* **133**, 13810–13813 (2011)
11. Wytenbach, T., Bowers, M.T.: Structural stability from solution to the gas phase: native solution structure of ubiquitin survives analysis in a solvent-free ion mobility–mass spectrometry environment. *J. Phys. Chem. B.* **115**, 12266–12275 (2011)
12. May, J.C., Goodwin, C.R., Lareau, N.M., Leaprot, K.L., Morris, C.B., Kurulugama, R.T., Mordehai, A., Klein, C., Barry, W., Darland, E., Overmyer, G., Imatani, K., Stafford, G.C., Fjeldsted, J.C., McLean, J.A.: Conformational ordering of biomolecules in the gas phase: nitrogen collision cross sections measured on a prototype high resolution drift tube ion mobility-mass spectrometer. *Anal. Chem.* **86**, 2107–2116 (2014)
13. Zhong, Y., Han, L., Ruotolo, B.T.: Collisional and coulombic unfolding of gas-phase proteins: high correlation to their domain structures in solution. *Angew. Chemie Int. Ed.* **53**, 9209–9212 (2014)

14. Wamke, S., Baldauf, C., Bowers, M.T., Pagel, K., von Helden, G.: Photodissociation of conformer-selected ubiquitin ions reveals site-specific cis/trans isomerization of proline peptide bonds. *J. Am. Chem. Soc.* **136**, 10308–10314 (2014)
15. Polfer, N.C., Oomens, J.: Vibrational spectroscopy of bare and solvated ionic complexes of biological relevance. *Mass Spectrom. Rev.* **28**, 468–494 (2009)
16. Periasamy, A.: Fluorescence resonance energy transfer microscopy: a mini review. *J. Biomed. Opt.* **6**, 287–291 (2001)
17. Forbes, M.W., Jockusch, R.A.: Gas-phase fluorescence excitation and emission spectroscopy of three xanthene dyes (rhodamine 575, rhodamine 590 and rhodamine 6G) in a quadrupole ion trap mass spectrometer. *J. Am. Soc. Mass Spectrom.* **22**, 93–109 (2011)
18. Czar, M.F., Zosel, F., König, I., Nettels, D., Wunderlich, B., Schuler, B., Zarrine-Afsar, A., Jockusch, R.A.: Gas-phase FRET efficiency measurements to probe the conformation of mass-selected proteins. *Anal. Chem.* **87**, 7559–7565 (2015)
19. Dashtiev, M., Azov, V., Frankevich, V., Scharfenberg, L., Zenobi, R.: Clear evidence of fluorescence resonance energy transfer in gas-phase ions. *J. Am. Soc. Mass Spectrom.* **16**, 1481–1487 (2005)
20. Hendricks, N.G., Julian, R.R.: Leveraging ultraviolet photodissociation and spectroscopy to investigate peptide and protein three-dimensional structure with mass spectrometry. *Analyst* **141**, 4534–4540 (2016)
21. Daly, S., Poussiguet, F., Simon, A.-L., MacAleese, L., Bertorello, F., Chirot, F., Antoine, R., Dugourd, P.: Action-FRET: probing the molecular conformation of mass-selected gas-phase peptides with Förster resonance energy transfer detected by acceptor-specific fragmentation. *Anal. Chem.* **86**, 8798–8804 (2014)
22. Daly, S., Knight, G., Halim, M.A., Kulesza, A., Choi, C.M., Chirot, F., MacAleese, L., Antoine, R., Dugourd, P.: Action-FRET of a gaseous protein. *J. Am. Soc. Mass Spectrom.* **28**, 38–49 (2017)
23. Hendricks, N.G., Lareau, N.M., Stow, S.M., McLean, J.A., Julian, R.R.: Bond-specific dissociation following excitation energy transfer for distance constraint determination in the gas phase. *J. Am. Chem. Soc.* **136**, 13363–13370 (2014)
24. Hendricks, N.G., Julian, R.R.: Characterizing gaseous peptide structure with action-EET and simulated annealing. *Phys. Chem. Chem. Phys.* **17**, 25822–25827 (2015)
25. Hendricks, N.G., Julian, R.R.: Two-step energy transfer enables use of phenylalanine in action-EET for distance constraint determination in gaseous biomolecules. *Chem. Commun.* **51**, 12720–12723 (2015)
26. Scutelnic, V., Prlj, A., Zabuga, A., Corminboeuf, C., Rizzo, T.R.: Infrared spectroscopy as a probe of electronic energy transfer. *J. Phys. Chem. Lett.* **9**, 3217–3223 (2018)
27. Talbert, L.E., Julian, R.R.: Directed-backbone dissociation following bond-specific carbon-sulfur UVPD at 213 nm. *J. Am. Soc. Mass Spectrom.* **29**, 1760–1767 (2018)
28. Diedrich, J.K., Julian, R.R.: Facile identification of phosphorylation sites in peptides by radical directed dissociation. *Anal. Chem.* **83**, 6818–6826 (2011)
29. Diedrich, J.K., Julian, R.R.: Site-selective fragmentation of peptides and proteins at quinone-modified cysteine residues investigated by ESI-MS. *Anal. Chem.* **82**, 4006–4014 (2010)
30. Soares, M.S.P., Oliveira, P.S., Debom, G.N., da Silveira Mattos, B., Polachini, C.R., Baldissarelli, J., Morsch, V.M., Schetinger, M.R.C., Tavares, R.G., Stefanello, F.M., Spanevello, R.M.: Chronic administration of methionine and/or methionine sulfoxide alters oxidative stress parameters and ALA-D activity in liver and kidney of young rats. *Amino Acids* **49**, 129–138 (2017)
31. Hamdy, O.M., Alizadeh, A., Julian, R.R.: The innate capacity of proteins to protect against reactive radical species. *Analyst* **140**(15), 5023–5028 (2015)
32. Hatfield, D., Diamond, A.: UGA: a split personality in the universal genetic code. *Trends Genet.* **9**, 69–70 (1993)
33. Bertsson, R.P.-A., Alia Oktaviani, N., Fusetti, F., Thunnissen, A.-M.W.H., Poolman, B., Slotboom, D.-J.: Selenomethionine incorporation in proteins expressed in *Lactococcus lactis*. *Protein Sci.* **18**, 1121–1127 (2009)
34. Barton, W.A., Tzvetkova-Robev, D., Erdjument-Bromage, H., Tempst, P., Nikolov, D.B.: Highly efficient selenomethionine labeling of recombinant proteins produced in mammalian cells. *Protein Sci.* **15**, 2008–2013 (2006)
35. Wessjohann, L.A., Schneider, A., Abbas, M., Brandt, W.: Selenium in chemistry and biochemistry in comparison to sulfur. *Biol. Chem.* **388**, 997 (2007)
36. Reich, H.J., Hondal, R.J.: Why nature chose selenium. *ACS Chem. Biol.* **11**, 821–841 (2016)
37. Chan, W.C., White, P.D.: Fmoc solid phase peptide synthesis: a practical approach. (2004)
38. Rossi, M., Blum, V., Kupser, P., von Helden, G., Bierau, F., Pagel, K., Meijer, G., Scheffler, M.: Secondary structure of Ac-Alan-LysH⁺ polyalanine peptides (n = 5,10,15) in Vacuo: helical or not? *J. Phys. Chem. Lett.* **1**, 3465–3470 (2010)
39. Bossio, R.E., Hudgins, R.R., Marshall, A.G.: Gas phase photochemistry can distinguish different conformations of unhydrated photoaffinity-labeled peptide ions. *J. Phys. Chem. B.* **107**, 3284–3289 (2003)
40. Mach, H., Sanyal, G., Volkin, D.B., Middaugh, C.R.: Applications of ultraviolet absorption spectroscopy to the analysis of biopharmaceuticals. In: *Therapeutic Protein and Peptide Formulation and Delivery*, pp. 11–186. American Chemical Society (1997) 10.1021/bk-1997-0675.ch011
41. Hudgins, R.R., Jarrold, M.F.: Helix formation in unsolvated alanine-based peptides: helical monomers and helical dimers. *J. Am. Chem. Soc.* **121**(14), 3494–3501 (1999)
42. Ouerdane, L., Mester, Z.: Production and characterization of fully selenomethionine-labeled *Saccharomyces cerevisiae*. *J. Agric. Food Chem.* **56**, 11792–11799 (2008)